JAST, Vol. 4, No. 3, pp 37–43

JAST
Journal of Aerospace Science and Technology

RESEARCH NOTE

Vibration and Critical Speed of Axially loaded Rotating Orthotropic Cylindrical Shells

K. Daneshjou[1], M. Talebitooti[2], R. Talebitooti[3]

In this paper, classical thin shell theory is used to analyze vibration and critical speed of simply supported rotating orthotropic cylindrical shells. The effects of centrifugal and Coriolis forces due to the rotation are considered in the present formulation. In addition, axial load is applied to cylinder as a ratio of critical buckling load. Finally the effects of orthotropic ratio, material and geometry of the shell as well as axial loads on bifurcation of natural frequency are investigated.

INTRODUCTION

The critical speed analysis of shaft-disk systems has been extensively investigated in the last hundred years whereas similar analyses on cylindrical shells or drum-like rotor structures have been few and far between. Rotating cylindrical shells are used in many industrial applications such as gas turbine engines, electric motors, rotary kiln and rotor systems. The orthotropic cylindrical shell is extensively used in mechanical structures, such as aircraft fuselages, missiles, and submarines, *etc.* Hence, vibration characteristics of rotating orthotropic cylindrical shells are of great importance. The rotating cylindrical shells can be fatigued by lower speed than the design speed. Therefore, one should analyze the vibration characteristics of the rotating shell to obtain the stability and reliability.

The first published work on this problem was by Bryan [1], in which a rotating thin ring was considered and it was here that the phenomena of traveling modes were discovered. The effects of Coriolis forces were first investigated by DiTaranto and Lessen [2] for an infinitely long, isotropic cylindrical shell. Srinivasan and Lauterbach [3] later combined both the effects of Coriolis forces and travelling modes in the study of rotating isotropic cylindrical shells. However, these three articles concentrated mainly on natural frequency analysis.

The first critical speed results for rotating shells were obtained experimentally by Zinberg and Symonds [4]. The results also proved the advantages of using shells made of orthotropic materials over aluminum alloy shells. A finite element approach was used by dos Reis *et. al.* [5] to obtain the critical speeds in the evaluation of the shell of Zinberg and Symonds [4]. A simplified theory for analyzing the first critical speed of a composite cylindrical shell was performed by Kim and Bert [6]. Results obtained using various shell theories were compared. The vibration and critical speed of thin, isotropic cylindrical shells under constant axial loads is studied by Ng and Lam [7]. Haung and Chen used a modified receptance method for the vibration analysis of rotating cylindrical shells with internal, symmetric as well as external ring stiffeners [8]. Lee and Kim used the energy method to examine the effect of boundary conditions on the free vibration of rotating composite cylindrical shells with orthogonal stiffeners [9,10]. Lam and Loy [11] also compared the natural frequencies of rotating laminated cylindrical shells with different shell theories, namely Donnell's, Flugge's, Love's and Sanders'.

Liew *et. al.* [12] proposed the harmonic reproducing kernel particle method for the free vibration analysis of rotating cylindrical shells. The effects of centrifugal and Coriolis forces as well as the initial hoop tension due to rotation are all taken into account. Zhao *et. al.* [13] presented the free vibration analysis of simply supported rotating cross-ply laminated cylindrical

1. *Professor, Dept. of Mechanical Eng., Iran Univ. of Science and Tech., Tehran, Iran.*
2. *MSc. Student, Dept. of Mechanical Eng., Isfahan Univ. of Tech., Isfahan, Iran.*
3. *Ph.D. Candidate, Dept. of Mechanical Eng., Iran Univ. of Science and Tech., Tehran, Iran, Email: rtalebi@iust.ac.ir.*

shells with axial and circumferential stiffeners using an energy approach.

In most publications on critical speeds of rotating cylindrical shells, the effects of axial loadings on the critical speed characteristics of orthotropic shell are not found. In this paper, a theoretical analysis is presented to study the critical speeds of rotating orthotropic cylindrical shells under axial loadings. The analysis is carried out using Sanders theory for thin shells together with consideration of the initial hoop tension and centrifugal and Coriolis forces. The problem is formulated to allow the cylindrical shell any boundary conditions but for simplicity, results are presented only for the case of simply-supported shells as the displacement fields which satisfy these boundary conditions can easily be expressed in terms of the products of sine and cosine functions.

THEORY AND FORMULATION

The cylindrical shell under consideration is with constant thickness h, radius R and length L, rotating about the x-axis at constant angular velocity Ω. The reference surface of the shell is taken to be at its middle surface where an orthogonal co-ordinate system (x, θ, z) is fixed. The x co-ordinate is taken in the axial direction of the shell, where the θ and z co-ordinates are respectively in the circumferential and radial directions of the shell as shown in Figure 1. The deformations of the cylinder are defined by u, v, w in the x, θ, z directions respectively. The elastic modulus in axial and circumferential directions are denoted by E_z, E_θ and corresponding Poisson's ratio by ν_z, ν_θ respectively. Also mass density is denoted by ρ and the constant extensional axial load per unit length by N_x. For an orthotropic shell the stress-strain equations are:

$$\epsilon_z = \frac{1}{E_z}\left(\sigma_z - \nu_z\,\sigma_\theta\right) \tag{1}$$

$$\epsilon_\theta = \frac{1}{E_\theta}\left(\sigma_\theta - \nu_\theta\,\sigma_z\right) \tag{2}$$

$$\gamma_{z\theta} = \frac{\tau_{z\theta}}{G} \tag{3}$$

which, when inverted, become:

$$\sigma_z = \frac{1}{1-\nu_z\,\nu_\theta}\left(E_z\,\epsilon_z + \nu_z\,E_\theta\,\epsilon_\theta\right) \tag{4}$$

$$\sigma_\alpha = \frac{1}{1-\nu_z\,\nu_\theta}\left(E_\theta\,\epsilon_\theta + \nu_\theta\,E_z\,\epsilon_z\right) \tag{5}$$

$$\tau_{z\theta} = G\,\gamma_{z\theta} \tag{6}$$

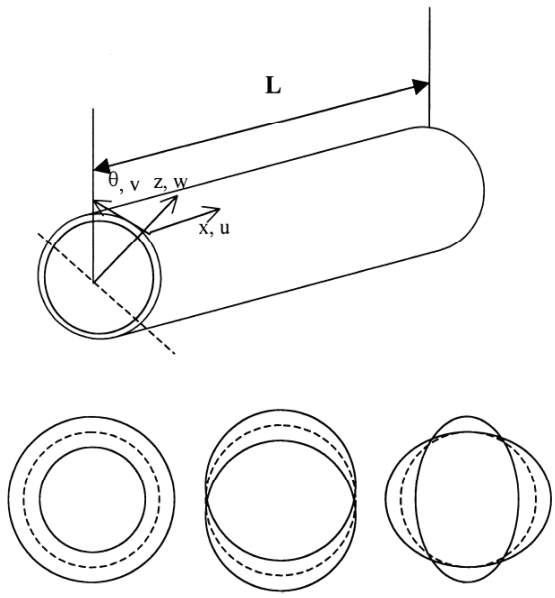

Figure 1. Co-ordinate system, circumferential modal shape.

However, the five elastic constants E_α, E_β, γ_α, ν_β and G are not independent; symmetry consideration requires that:

$$\nu_\alpha E_\beta = \nu_\beta E_\alpha \tag{7}$$

The equations of motion for a orthotropic cylindrical shell can be written [14] as:

$$\left[L_{D-M} + K_D\,L_{Mod,Sander} + (1/C)L_{\text{int}}\right]\{u, \nu, w\}' = \vec{g} \tag{8}$$

where $K_D = h^2/12R^2$, $C = Eh/(1-\nu_\alpha\nu_\beta)$ and $\vec{g}$ is defined as:

$$\vec{g} = \frac{\rho h R^2}{c_{22}}\begin{Bmatrix} \frac{\partial^2 u}{\partial t^2} \\ \frac{\partial^2 v}{\partial t^2} + 2\Omega\frac{\partial w}{\partial t} - \Omega^2 v \\ \frac{\partial^2 w}{\partial t^2} - 2\Omega\frac{\partial v}{\partial t} - \Omega^2 w \end{Bmatrix} \tag{9}$$

$[L_{D-M}]$, $[L_{Mod,Sander}]$ are the Donnell-Mushtari and modifying Sanders operator, respectively, and $[L_{\text{int}}]$ is a matrix operator containing the additional terms which account for initial stresses. Donnell-Mushtari operator is defined as:

$$[L_{D-M}] = \begin{bmatrix} a_{11} & a_{12} & a_{13} \\ a_{21} & a_{22} & a_{23} \\ a_{31} & a_{32} & a_{33} \end{bmatrix} \tag{10}$$

where

$$a_{11} = \frac{C_{11}}{C_{22}}\frac{\partial^2}{\partial s^2} + 2\frac{C_{16}}{C_{22}}\frac{\partial^2}{\partial s\,\partial\theta} + \frac{C_{66}}{C_{22}}\frac{\partial^2}{\partial\theta^2} \tag{11}$$

$$a_{22} = \frac{C_{66}}{C_{22}}\frac{\partial^2}{\partial s^2} + 2\frac{C_{66}}{C_{22}}\frac{\partial^2}{\partial s\,\partial\theta} + \frac{\partial^2}{\partial\theta^2} \tag{12}$$

$$a_{33}=1+K_D\left[\frac{D_{11}}{D_{22}}\frac{\partial^4}{\partial\delta^4}+2\left(\frac{D_{12}+2D_{66}}{D_{22}}\right)\frac{\partial^4}{\partial s^2\,\partial\theta^2}+\frac{\partial^4}{\partial\theta^4}\right] \tag{13}$$

$$a_{12}=a_{21}=\frac{C_{16}}{C_{22}}\frac{\partial^2}{\partial s^2}+\left(\frac{C_{12}+C_{66}}{C_{22}}\right)\frac{\partial^2}{\partial s\,\partial\theta}+\frac{C_{26}}{C_{22}}\frac{\partial^2}{\partial\theta^2} \tag{14}$$

$$a_{13}=a_{31}=\frac{C_{12}}{C_{22}}\frac{\partial}{\partial s}+\frac{C_{26}}{C_{22}}\frac{\partial}{\partial\theta} \tag{15}$$

$$a_{23}=a_{32}=\frac{C_{26}}{C_{22}}\frac{\partial}{\partial s}+\frac{\partial}{\partial\theta} \tag{16}$$

where $s = x/R$; C_{11}, C_{12}, C_{22} and C_{66} are the extensional stiffness constants defined by:

$$C_{11}=\frac{E_\alpha h}{1-\nu_\alpha\,\nu_\beta},\qquad C_{22}=\frac{E_\beta h}{1-\nu_\alpha\,\nu_\beta} \tag{17}$$

$$C_{12}=\frac{\nu_\alpha E_\beta h}{1-\nu_\alpha\,\nu_\beta}=\frac{\nu_\beta E_\alpha h}{1-\nu_\alpha\,\nu_\beta}, \tag{18}$$

$$C_{66}=Gh \tag{19}$$

and D_{11}, D_{12}, D_{22} and D_{66} are the bending stiffness constants defined by:

$$D_{11}=\frac{E_\alpha h^3}{12(1-\nu_\alpha\,\nu_\beta)},\quad D_{22}=\frac{E_\beta h^3}{12(1-\nu_\beta\,\nu_\alpha)} \tag{20}$$

$$D_{12}=\frac{\nu_\alpha E_\beta h^3}{12(1-\nu_\alpha\,\nu_\beta)}=\frac{\nu_\beta E_\alpha h^3}{12(1-\nu_\alpha\,\nu_\beta)} \tag{21}$$

$$D_{66}=\frac{Gh^3}{12} \tag{22}$$

Modifying Sanders operator is defined as:

$$L_{Mod,\,Sander}=\begin{bmatrix}b_{11}&b_{12}&b_{13}\\b_{21}&b_{22}&b_{23}\\b_{31}&b_{32}&b_{33}\end{bmatrix} \tag{23}$$

where

$$b_{11}=\frac{1}{4}\,\frac{D_{66}}{D_{22}}\,\frac{\partial^2}{\partial\theta^2} \tag{24}$$

$$b_{22}=\frac{9}{4}\,\frac{D_{66}}{D_{22}}\,\frac{\partial^2}{\partial s^2}+3\frac{D_{26}}{D_{22}}+\frac{\partial^2}{\partial\theta^2} \tag{25}$$

$$b_{33}=4\,\frac{D_{16}}{D_{22}}\,\frac{\partial^4}{\partial\delta^3\,\partial\theta}+4\frac{D_{26}}{D_{22}}\,\frac{\partial^4}{\partial s\,\partial\theta^3} \tag{26}$$

$$b_{12}=b_{21}=\frac{-3}{4}\,\frac{D_{66}}{D_{22}}\,\frac{\partial^2}{\partial s\,\partial\theta}-\frac{1}{2}\,\frac{D_{26}}{D_{22}}\,\frac{\partial^2}{\partial\theta^2} \tag{27}$$

$$b_{13}=b_{31}=\frac{1}{2}\,\frac{D_{16}}{D_{22}}\,\frac{\partial^3}{\partial s^2\,\partial\theta}+\frac{D_{66}}{D_{22}}\,\frac{\partial^3}{\partial s\,\partial\theta^2}+\frac{1}{2}\,\frac{D_{26}}{D_{22}}\,\frac{\partial^3}{\partial\theta^3} \tag{28}$$

$$b_{23}=b_{32}=\frac{-3}{2}\,\frac{D_{16}}{D_{22}}\,\frac{\partial^3}{\partial s^3}-\left(\frac{D_{12}+3D_{66}}{D_{22}}\right)\frac{\partial^3}{\partial s^2\,\partial\theta}-\frac{7}{2}\,\frac{D_{26}}{D_{22}}\,\frac{\partial^3}{\partial s\,\partial\theta^2}-\frac{\partial^3}{\partial\theta^3} \tag{29}$$

and for initial stresses we have:

$$L_{\text{int}}=\begin{bmatrix}i_{11}&i_{12}&i_{13}\\i_{21}&i_{22}&i_{23}\\i_{31}&i_{32}&i_{33}\end{bmatrix} \tag{30}$$

where:

$$i_{11}=\frac{\partial}{\partial\theta}\left(\frac{N_x}{4}\,\frac{\partial}{\partial\theta}\right)+\frac{N_\theta}{4}\,\frac{\partial^2}{\partial\theta^2} \tag{31}$$

$$i_{22}=-\frac{\partial}{\partial s}\left[\frac{1}{4}\,(N_x+N_\theta)\,\frac{\partial}{\partial s}\right]-N_\theta \tag{32}$$

$$i_{33}=-\frac{\partial}{\partial s}\left(N_x\frac{\partial}{\partial s}\right)-N_\theta\frac{\partial^2}{\partial\theta^2}-\frac{\partial}{\partial s}\left(N_{x\theta}\frac{\partial}{\partial\theta}\right)-N_{x\theta}\frac{\partial^2}{\partial s\,\partial\theta} \tag{33}$$

$$i_{12}=-\frac{\partial}{\partial\theta}\left(\frac{N_x}{4}\,\frac{\partial}{\partial s}\right)-\frac{N_\theta}{4}\,\frac{\partial^2}{\partial s\,\partial\theta} \tag{34}$$

$$i_{21}=-\frac{\partial}{\partial s}\left[\frac{1}{4}\,(N_x+N_\theta)\,\frac{\partial}{\partial\theta}\right] \tag{35}$$

$$i_{23}=N_\theta\frac{\partial}{\partial\theta}+N_{x\theta}\frac{\partial}{\partial s} \tag{36}$$

$$i_{32}=N_\theta\frac{\partial}{\partial\theta}+2N_{x\theta}\frac{\partial}{\partial s}+\frac{\partial N_{x\theta}}{\partial s} \tag{37}$$

$$i_{13} = i_{31} = 0 \tag{38}$$

where $N_{x\theta} = 0$ and The initial hoop tension due to the centrifugal force is defined as:

$$N_\theta = \rho\, h\, \Omega^2 R^2 \tag{39}$$

If the shell assumed is simply supported, there exists a solution for the above three equations in the form:

$$u = A\cos\frac{m\pi x}{L}\cos(\omega t + n\theta) \tag{40}$$

$$v = B\sin\frac{m\pi x}{L}\sin(\omega t + n\theta) \tag{41}$$

$$w = C\sin\frac{m\pi x}{L}\cos(\omega t + n\theta) \tag{42}$$

where n represents the number of circumferential waves and m the number of axial half-waves in the corresponding standing wave pattern. Eq. (8) is solved using an eigenfunction expansion in terms of the normal modes of the free vibrations of a cylindrical shell. Substitution of Eqs. (40-42) into Eq. (8) yields a set of three coupled homogenous equations.

$$\begin{bmatrix} M_{11} & M_{12} & M_{13} \\ M_{21} & M_{22} & M_{23} \\ M_{31} & M_{32} & M_{33} \end{bmatrix} \begin{Bmatrix} A \\ B \\ C \end{Bmatrix} = \begin{Bmatrix} 0 \\ 0 \\ 0 \end{Bmatrix} \tag{43}$$

Imposing non-trivial conditions on Eq. (43), the characteristic frequency equation is obtained by equating the determinant of the characteristic matrix in Eq. (45) to zero.

$$\beta_1\omega_{mn}^6 + \beta_2\omega_{mn}^4 + \beta_3\omega_{mn}^3 + \beta_4\omega_{mn}^2 + \beta_5\omega_{mn} + \beta_6 = 0 \tag{44}$$

Matlab Toolbox is used to solve six roots of Eq. for each m and n.

NUMERICAL RESULTS

The theoretical model developed can be used very effectively in the basic design stage of cylinder-shape in rotating systems. As a demonstration of such applications, design parameter studies are conducted. Numerical results have been generated for a cylindrical shell, with $L/R = 20$, $R/h = 50$ and different ratios of $OR_x = E_\theta/E_z$ when $(E_\theta = const)$ and $OR_y = E_\theta/E_z$ when $(E_z = const)$. The modes of interest here are the transverse modes as they correspond to the lowest two natural frequencies. The two higher axial and circumferential modes are not presented.

The critical speed phenomena can be clearly illustrated in Figure 2. The bifurcations of the natural frequencies for the transverse modes of $(m,n) = (1,1),(1,2),(1,3)$ for the shell of $OR_x = 0.5$ and

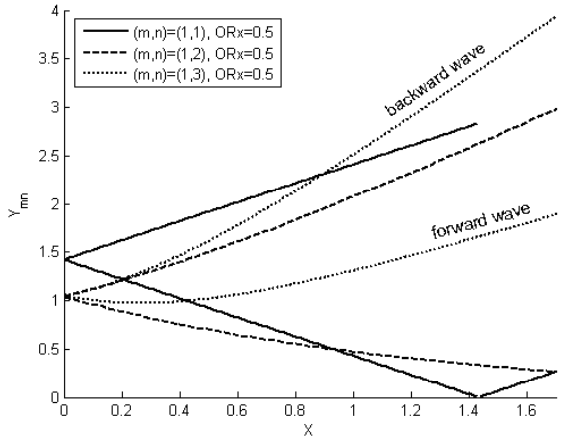

Figure 2. Bifurcations of natural frequencies of a rotating cylindrical shell of $L/R = 20, R/h = 50, OR_x = 0.5$.

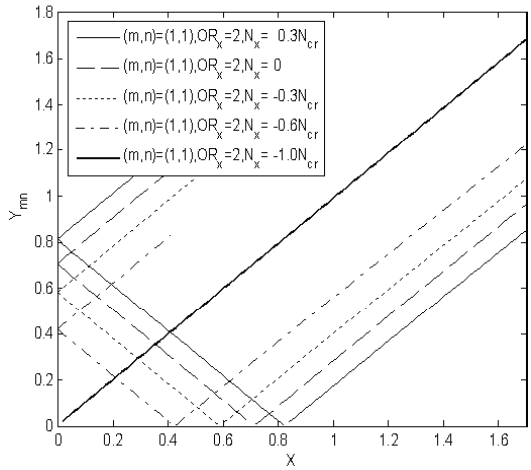

Figure 3. Bifurcations of natural frequencies of a rotating cylindrical shell of $L/R = 20, R/h = 50, OR_x = 2, (m,n) = (1,1)$ with different axial load.

without axial loading are presented. In the figure, Y_{mn} and X denote the normalized natural frequency (ω_{mn}) and rotational speed (Ω) respectively normalized with respect to the non-rotational natural frequency of ratio $OR_x = 1$ (isotropic shell) ω_{mno}.

$$Y_{mn} = \frac{\omega_{mn}}{\omega_{mno}} \tag{45}$$

$$X = \frac{\Omega}{\omega_{mno}} \tag{46}$$

Due to the Coriolis acceleration, the nodal lines are neither stationary nor rotating at the same angular velocity as the shell. It can be shown that each mode rotates at its own speed given by $\Omega - \omega_{mn}/n$ with respect to a stationary coordinate. The lower branch corresponds to the forward whirl and the upper branch corresponds to the backward whirl.

The critical speed of the rotating shell which occurs for mode $(1,1)$ corresponds to the rotational

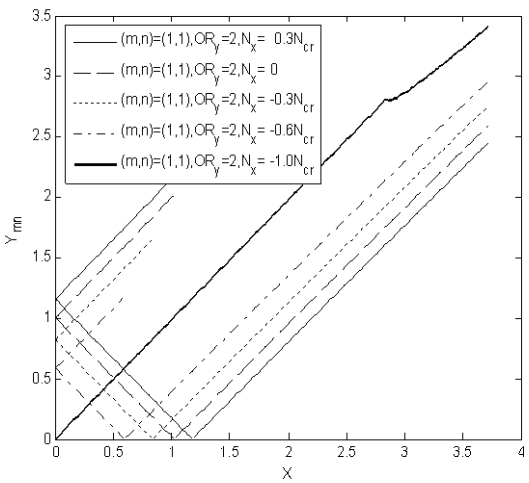

Figure 4. Bifurcations of natural frequencies of a rotating cylindrical shell of $L/R = 20, R/h = 50, OR_y = 2, (m,n) = (1,1)$ with different axial load.

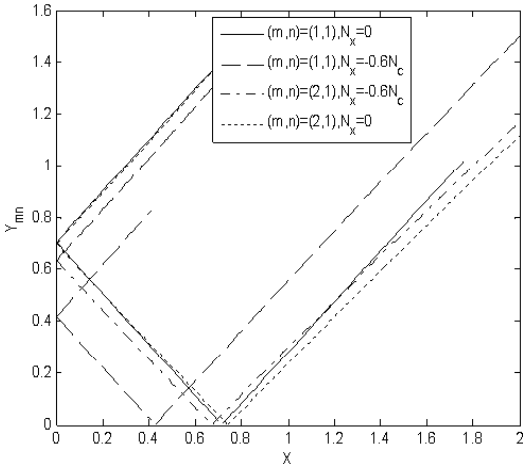

Figure 5. Sensitivity of natural frequencies of a rotating cylindrical shell $L/R = 20, R/h = 50, OR_x = 2$ to axial loads.

speed of the shell at which the forward mode intersects the abscissa. At this inter-section, possible unstable phenomenon exists as the forward mode becomes standing with respect to the traveling coordinate and is ready to switch to a backward mode. At this critical speed, any residual unbalance will synchronize with the rotation and magnify the whirling amplitude. Also, as seen in Figure 2 $(m,n) = (1,1)$ has a linear rate, whereas for $(m,n) = (1,2),(1,3)$ the nonlinearity is increased.

It is important to note here that the axial loading, if compressive, must be a fraction of the static critical buckling load, N_c. The governing buckling differential equations can be obtained by neglecting terms involving N_c, t and Ω, in Eq. (8). The buckling loads can be easily obtained by computing the eigenvalues of the resulting characteristic matrix. For the shell used in Figure 3 and Figure 4, the static critical buckling load, N_c, corresponds to the transverse mode of $(1,1)$ of ratios $OR_x = OR_y = 1$ (isotropic one). These figures show the bifurcations of the natural frequencies for the transverse mode of $(m,n) = (1,1)$ subjected to different axial loads. The response to tensile loading is generally predictable for all the modes with an upward shift for all the branches. This can be expected as tensile loading, which causes the shell to become stiffer. For compressive loadings, the expected downward shifts for all the branches are also observed. Also higher compressive loads make critical speed phenomenon occur in lower speed. Whenever the load approaches critical buckling load the bifurcations of natural frequencies are canceled. Two modes of interest, $(m,n) = (1,1)$ and $(2,1)$, are used to investigate the sensitivity of natural frequencies to axial loads. Figure 5 shows that different modes include different levels of sensitivity to the axial loadings.

It can be deduced that the level of sensitivity of a particular mode is proportionally dependent on the magnitude of the buckling load of that mode. For example, mode $(2,1)$ which has the highest buckling

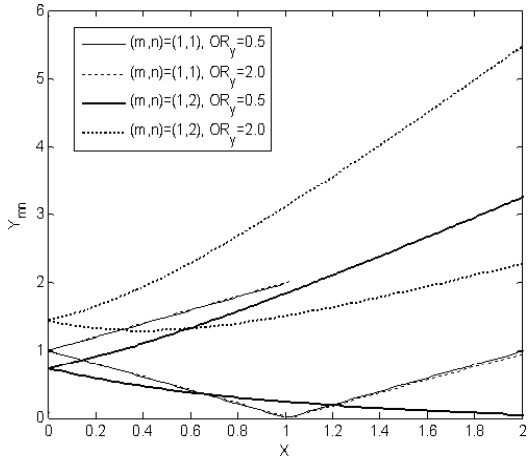

Figure 6. Sensitivity of two interest modes of a rotating cylindrical shell $L/R = 20$, $R/h = 50$, to ratio OR_y.

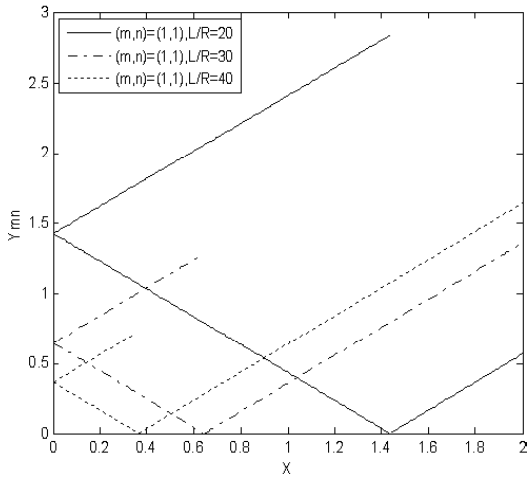

Figure 7. Sensitivity of natural frequencies of a rotating cylindrical shell $R/h = 50, N_x = 0, OR_x = 0.5$ to L/R.

load is observed to be the least sensitive, and mode $(1,1)$ whose buckling load is the critical buckling load, is observed to be the most sensitive.

To investigate how the effect of increase in stiffness can improve the natural frequency of rotating cylinder, especially in higher circumferential numbers (n), the Figure 6 is illustrated. As shown no significant difference can be observed comparing ratios $OR_y = 0.5, 2.0$ for $(m,n) = (1,1)$, whereas, at mode $(m,n) = (1,2)$ natural frequency is increased due to increase of circumferential mode number (n).

In Figure 7 the natural frequencies of the shell for miscellaneous $L/R = 20, 30, 40$ are illustrated. As shown, increasing this ratio decreases the natural frequency. It is also depicted that as a result of this growth, the critical speed shifts downwards to the power 2.

In Figure 8 the natural frequencies of the shell are investigated for different ratios of $R/h = 50, 100, 200$. It is well anticipated that when the ratio R/h shows the increase of 100%, the critical frequencies reduce by 50%. It is due to the fact that the shell stiffness changes at the same rate as the thickness.

Different orthotropic materials are used (Table 1), in order to investigate the properties of orthotropic material on bifurcations of natural frequencies of modes $(1,2)$.

Figure 9 shows that material should be chosen properly to enhance critical frequency. The axial and circumferential modulus ratios play a significant role. That is why the natural frequencies of Graphite Epoxy make the critical speed higher than the others. It is observed that in high rotating speeds, all materials behave the same approach except Fiber Epoxy. Also critical buckling load of Fiber Epoxy occurs in mode $(2,2)$ but the others in mode $(1,2)$. In addition it should be noted that, in spite of the highest axial module in Carbon, it is well observed that the critical speed of Carbon material is at the lowest.

CONCLUDING REMARKS

Bifurcation of natural frequency for axially loaded rotating orthotropic cylindrical shells, was investigated. The critical speed of the rotating shell which occurred for mode $(1,1)$ corresponded to the rotational speed of the shell at which the forward mode intersects the abscissa. In addition $(m,n) = (1,1)$ behaves a linear rate, whereas for $(m,n) = (1,2), (1,3)$ the nonlinearity was depicted. The significant increase of natural frequency due to increase of circumferential number (n) were observed. Also, the shell was subjected to axial load. Subsequently, tensile loading caused the shell to become stiffer, resulting in shifting upward of bifurcation, whereas, for compressive loadings, the expected downward shifts for all the branches were observed. On the other hand, higher compressive loads

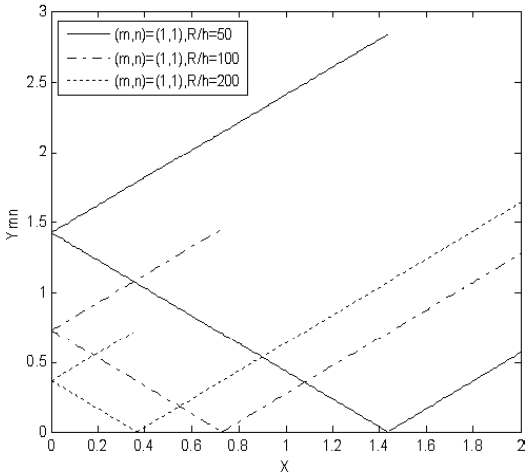

Figure 8. Sensitivity of natural frequencies of a rotating cylindrical shell $R/h = 50, N_x = 0, OR_x = 2$ to R/h.

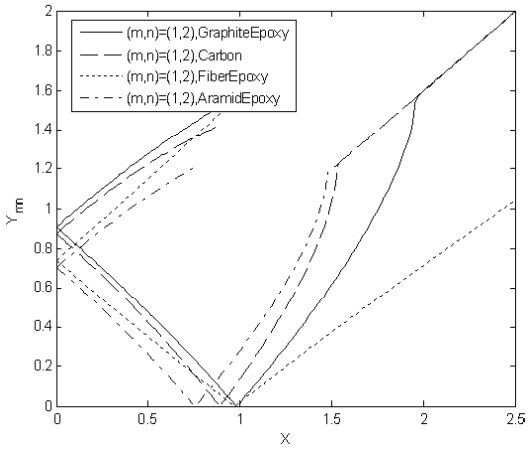

Figure 9. Bifurcations of natural frequencies of a rotating cylindrical shell of different orthotropic material $L/R = 20, R/h = 50$ at mode (1,2).

Table 1. Orthotropic Materials.

Name	Graphite Epoxy	Carbon	Fiberglass Epoxy	Aramid Epoxy
Density (kg/m^3)	1600	1600	1900	1500
E_1 (GPa)	125	324	56	76
E_2 (GPa)	10	5.86	13	5.5
ν_z	0.4	0.33	0.26	0.34
G_{12} (GPa)	5.9	1.1	4.2	2.3

caused critical speed phenomenon at a lower speed. Moreover, Bifurcations of natural frequencies were canceled where the buckling load applied to cylinder. Finally, Different orthotropic materials were compared, and results indicated that the natural frequencies of Graphite Epoxy are in the highest level.

REFERENCES

1. Bryan GH., "On the Beats in the Vibration of Revolving Cylinder or Bell", *Proceedings of the Cambridge Philosophical Society 7*, PP 101-111(1890).
2. DiTaranto RA., Lessen M., "Coriolis Acceleration Effect on the Vibration of a Thin-Walled Circular Cylinder", *ASME Journal of Applied Mechanics*, **31**, PP 700-701(1964).
3. Srinivasan AV., Lauterbach GF., "Traveling Waves in Rotating Cylindrical Shells", *ASME Journal of Engineering for Industry*, **93**, PP 1229-1232(1971).
4. Zinberg H., Symonds MF., "The Development of Advanced Composite Tail Rotor Driveshaft", *26th Annual Forum of the American Helicopter Society*, PP 1-14(1979).
5. Dos Reis H., Goldman R., Verstrate Ph., "Thin-Walled Laminated Composite Cylindrical Tubes: Part III - Critical Speed Analysis", *Journal of Composites Technology and Research*, **9**, PP 58-62(1987).
6. Kim CD., Bert CW., "Critical Speed Analysis of Laminated Composite, Hollow Drive Shafts", *Composite Engineering* , **3**(7-8), PP 633-643(1993).
7. Ng T.Y., Lam K.Y., "Vibration and Critical Speed of a Rotating Cylindrical Shell Subjected to Axial Loading", *Applied Acoustics*, **56**(4), PP 273-282(1999).
8. Huang S.C., Chen L.H., "Vibration of a Spinning Cylindrical Shell with Internal/External Ring Stiffeners", *ASME journal of Vibration and Acoustics*, **118**(2), PP 227-236(1996).
9. Lee Y.S., Kim Y.W., "Vibration Analysis of Rotating Composite Cylindrical Shells with Orthogonal Stiffeners", *Computers and Structures*, **69**(2), PP 271-281(1998).
10. Lee Y.S., Kim Y.W., "Effect of Boundary Conditions on Natural Frequencies for Rotating Composite Cylindrical Shells with Orthogonal Stiffeners", *Advanced Engineering Software*, **30**(9-11), PP 649-655(1999).
11. Lam KY., Loy CT., "Analysis of Rotating Laminated Cylindrical Shells by Different Thin Shell Theories", *Journal of Sound and Vibration*, **186**(1), PP 23-35(1995).
12. Liew K.M., Ng T.Y, Zhao X., Reddy J.N., "Harmonic Reproducing Kernel Particle Method for Free Vibration Analysis of Rotating Cylindrical Shells", *Computer Methods in Applied Mechanics and Engineering*, **191**(37), PP 4141-4157(2002).
13. Zhao X., Liew K.M., Ng T.Y., "Vibration of Rotating Cross-Ply Laminated Circular Cylindrical Shells with Stringer and Ring Stiffeners", *International Journal of Solids and Structures*, **39**(2), PP 529-545(2002).
14. Leissa W., *Vibration of Shells(NASA SP-288)*, Washington DC- US Government Printing Office, (1973).